



Versatile control of the optical bandgap in heterobimetallic polymers through complexation of bithiazole-containing polyplatinynes with $\text{ReCl}(\text{CO})_5$

Li Li^{a,b}, Cheuk-Lam Ho^{b,c}, Wai-Yeung Wong^{b,c,*}

^aJiangxi Key Laboratory of Functional Organic Molecules, Jiangxi Science & Technology Normal University, Nanchang, Jiangxi, PR China

^bDepartment of Chemistry and Institute of Advanced Materials, Hong Kong Baptist University, Waterloo Road, Kowloon Tong, Hong Kong, PR China

^cInstitute of Molecular Functional Materials, Areas of Excellence Scheme, University Grants Committee, Hong Kong, PR China

ARTICLE INFO

Article history:

Received 1 November 2011

Accepted 20 December 2011

Keywords:

Bithiazole
Metallopolymers
Platinum
Rhenium
Thiophene

ABSTRACT

A new class of soluble, solution-processable heterobimetallic platinum(II)-acetylide polymers functionalized with some rhenium(I)-bithiazole based spacers and their corresponding model complexes were synthesized and characterized. The photophysical (absorption and emission spectra), thermal and electrochemical properties of the polymers were investigated in detail. These mixed-metal PtRe polymers exhibited good thermal stability and strong low-energy broad absorption bands in the visible region. The effects of metal complexation of the bithiazole group with $\text{ReCl}(\text{CO})_5$ as well as adding thiophene ring along the polymer backbone on the optical bandgaps of these organometallic polymers were examined. The bandgaps of these polymers were found to be controllable readily by chemical means and can be lowered from 2.18 to 1.89 eV as the number of thiophene ring was increased from 0 to 2. Upon coordination with $\text{Re}(\text{CO})_3\text{Cl}$ moiety, the optical gap of the polymer can be reduced by as large as 0.25 eV.

© 2011 Elsevier B.V. All rights reserved.

1. Introduction

There is considerable interest in the chemistry of soluble conjugated organometallic polymers in view of their potential applications in solar/photovoltaic cells, field-effect transistors, light-emitting diodes or non-linear optics (NLO) [1–16]. While most of the studies have been concentrated on the homometallic system, there is an increasing attention on the development of heterometallic congeners because of the effect of electronic influence of the second metal center on their functional properties. For instance, a heterobimetallic platinum-acetylide polymer of ferrocenylfluorene **II** was reported and spectroscopically characterized [17]. The presence of significant donor-acceptor interaction in **II** leads to a narrow bandgap value of 2.10 eV for this Pt-Fe mixed-metal material, which is much lower than that for the parent mononuclear polymer **I** (Fig. 1). Polymer **II** is electroactive with the half-wave potential of the ferrocene moiety slightly more anodic in **II** than in the diethynyl ligand precursor, in line with the transfer of electron density from the peripheral ferrocenyl donor unit to the π -conjugated main chain.

Based on the recent development in organic polymers in which their bandgaps can be reduced by the copolymerization of donor and acceptor units [18–21], it was envisaged that metallo-diethynyl ligands would constitute an interesting new class of spacer units in the design of novel organometallic polyynne systems, leading to a significant difference in their electronic properties (e.g. the HOMO-LUMO energy or optical bandgap).

Since the discovery of double-layer organic light-emitting diodes (OLEDs) based on Alq_3 [tris-(8-quinolinolato)aluminium] as the emitting material by Tang and VanSlyke [22], intensive research has been focused on the design and synthesis of other metal-containing luminophores. The design of novel materials for OLED applications demands well-defined requirements in terms of emission wavelength (λ_{em}), lifetime (τ), and quantum yields (Φ) [23–31]. Therefore, the compounds containing d^6 metals such as rhenium(I) [32–34], iridium(III) [35–37] and osmium(II) [38,39] which show good phosphorescent emission and high Φ (theoretically up to 100%) compared to those of fluorescent materials have attracted growing interest. Many researchers have focused on a particularly important class of complexes with the type of *fac*- $[\text{Re}(\text{CO})_3(\text{N}-\text{N})(\text{X})]$, where $\text{N}-\text{N}$ = diimine and X = halides. This class of metal complexes affords good phosphorescent emitters, where the strong spin-orbit coupling would enhance the singlet-triplet mixing, giving a fairly long-lived excited state with high emission quantum efficiencies [34], for applications in OLEDs [40] and in other fields such as solar energy conversion [41], supramolecular chemistry [42], catalysis

* Corresponding author. Institute of Molecular Functional Materials, Areas of Excellence Scheme, University Grants Committee, Hong Kong, PR China. Tel.: +86 852 34117074; fax: +86 852 34117348.

E-mail address: rwywong@hkbu.edu.hk (W.-Y. Wong).

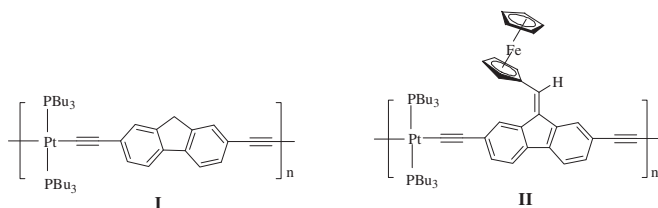


Fig. 1. Chemical structures of the polymers I and II.

[43], and medical chemistry [44]. Their peculiar molecular properties, and the possibilities of related technological applications, are directly related to the wide range of spectra of the molecules that determine the optical absorption and emission characteristics and the electronic structures of the ground as well as the lowest excited states in the molecules.

Much recent interest has been paid to the development of molecular and polymeric materials containing the bithiazole spacer [45–49]. It is known that poly(thiophene-2,5-diyl) and their derivatives are composed of “electron-donating” heterocyclic units (p-doping) whereas polymers such as poly(pyridine-2,5-diyl) contain “electron-withdrawing” imine group (n-doping) [50]. Incorporation of a thiazole unit, a hybrid of the thiophene and pyridine groups, in the main chain of the metallopolynes represents an attractive synthetic strategy to control the energy gap of this class of materials [51]. In the presence of electron-withdrawing imine nitrogen atoms, the optical spectra for the bithiazole derivatives typically display a significant red-shift when compared to their bithienyl counterparts [52]. However, the complexation reactions of bithiazole group with metal center was relatively less explored in the literature. Along this line, we have designed and prepared a series of rhenium(I)-diimine based diethynyl metalloligands, which can be used to furnish their corresponding platinum(II) metallopolyyne polymers. The photophysical, thermal and redox properties of these polymers have also been investigated in terms of the spacer chain length and the tricarbonylrhenium(I) unit.

2. Experimental

2.1. General information

Solvents were carefully dried and distilled from appropriate drying agents prior to use. Commercially available reagents were used without further purification unless otherwise stated. All reagents for the chemical syntheses were purchased from Aldrich or Acros Organics. Reactions and manipulations were carried out under an atmosphere of prepurified nitrogen using Schlenk techniques. All reactions were monitored by thin-layer chromatography (TLC) with Merck pre-coated glass plates. Flash column chromatography and preparative TLC were carried out using silica gel from Merck (230–400 mesh). Infrared spectra were recorded as CH_2Cl_2 solutions using a Perkin–Elmer Paragon 1000 PC or Nicolet Magna 550 Series II FTIR spectrometer, using CaF_2 cells with a 0.5 mm path length. Fast atom bombardment (FAB) mass spectra were recorded on a Finnigan MAT SSQ710 system. NMR spectra were measured in CDCl_3 on a Varian Inova 400 MHz FT-NMR spectrometer and chemical shifts are quoted relative to tetramethylsilane for ^1H and ^{13}C nuclei and H_3PO_4 for ^{31}P nucleus. The synthesis of **L0-2Br** to **L2-2Br**, **L0-2TMS** to **L2-2TMS** and **L0** to **L2** was carried out according to the literature method [53].

2.2. Physical measurements

UV/Vis spectra were obtained on an HP-8453 diode array spectrophotometer. The solution emission spectra and lifetimes of the

compounds were measured on a Photon Technology International (PTI) Fluorescence QuantaMaster Series QM1 spectrophotometer. The quantum yields were determined in degassed CH_2Cl_2 solutions at 293 K against quinine sulfate in 0.1 N H_2SO_4 ($\Phi = 0.54$) [54]. Cyclic voltammetry measurements were carried out at a scan rate of 50 mV s^{-1} using a eDAQ EA161 potentiostat electrochemical interface equipped with a thin film coated ITO covered glass working electrode, a platinum counter electrode and a Ag/AgCl (in 3 M KCl) reference electrode. The solvent in all measurements was deoxygenated MeCN, and the supporting electrolyte was $0.1 \text{ M } [^n\text{Bu}_4\text{N}]\text{BF}_4$. Thin polymer films were deposited on the working electrode by dip-coating in chlorobenzene solution (6 mg mL^{-1}). Where appropriate, the oxidation and reduction potentials were used to determine the HOMO and LUMO energy levels using the equations $E_{\text{HOMO}} = [-(E_{\text{onset, ox}} \text{ (vs. Ag/AgCl)} - E_{\text{onset (N.H.E. vs. Ag/AgCl)})] - 4.50 \text{ eV}$ and $E_{\text{LUMO}} = [-(E_{\text{onset, red}} \text{ (vs. Ag/AgCl)} - E_{\text{onset (N.H.E. vs. Ag/AgCl)})] - 4.50 \text{ eV}$, where the potentials for N.H.E. versus vacuum and N.H.E. versus Ag/AgCl are 4.50 and -0.22 V , respectively [55,56].

2.3. Preparation of compounds

2.3.1. Synthesis of **L0-Re** to **L2-Re**

Ligands **L0-Re** to **L2-Re** were prepared from **L0**, **L1** and **L2** by reacting each of them with rhenium(I) pentacarbonyl chloride, respectively. A typical procedure was given for **L0-Re**.

A mixture of **L0** (80 mg, 0.17 mmol) and $\text{ReCl}(\text{CO})_5$ (62 mg, 0.62 mmol) in ethanol (15 mL) was stirred at 60°C under a nitrogen atmosphere overnight. The solvent was removed on a rotary evaporator in *vacuo*. The crude product was purified by column chromatography on silica gel eluting with $\text{CH}_2\text{Cl}_2/n$ -hexane (2:1, v/v) to provide **L0-Re** (101 mg, 77%) as a red solid.

Spectral data: IR (KBr): $\nu(\text{C}=\text{O})$ 1906br, 2025, $\nu(\text{C}\equiv\text{C})$ 2102, $\nu(\text{C}\equiv\text{CH})$ 3299 cm^{-1} . ^1H NMR (400 MHz, CDCl_3): $\delta = 3.85$ (s, 2H, $\text{C}\equiv\text{CH}$), 3.20–3.14 (m, 4H, $\text{CH}_3\text{C}_5\text{H}_{10}\text{CH}_2\text{CH}_2\text{CH}_2$), 1.91–1.84 (m, 4H, $\text{CH}_3\text{C}_5\text{H}_{10}\text{CH}_2\text{CH}_2\text{CH}_2$), 1.50–1.45 (m, 4H, $\text{CH}_3\text{C}_5\text{H}_{10}\text{CH}_2\text{CH}_2\text{CH}_2$), 1.38–1.27 (m, 20H, $\text{CH}_3\text{C}_5\text{H}_{10}\text{CH}_2\text{CH}_2\text{CH}_2$), 0.87 (t, $J = 6.6 \text{ Hz}$, 6H, $\text{CH}_3\text{C}_5\text{H}_{10}\text{CH}_2\text{CH}_2\text{CH}_2$) ppm. ^{13}C NMR (100 MHz, CDCl_3): $\delta = 194.95$, 186.87 (CO), 164.84, 159.41, 117.03 (Ar), 90.86, 72.02 ($\text{C}\equiv\text{C}$), 31.94, 31.80, 29.65, 29.50, 29.38, 29.35, 29.09, 22.75, 14.22 (C_9H_{19}) ppm. FAB-MS (m/z): 774 [$\text{M} + 1$] $^+$, 739 [$\text{M}-\text{Cl}+1$] $^+$. Anal. Calc. For $\text{C}_{31}\text{H}_{40}\text{N}_2\text{ClO}_3\text{S}_2\text{Re}$: C, 48.08; H, 5.21; N, 3.62. Found: C, 48.19; H, 5.32; N, 3.70%.

L1-Re: Red solid (68%). **Spectral data:** IR (KBr): $\nu(\text{C}=\text{O})$ 1908, 1930, 2033, $\nu(\text{C}\equiv\text{C})$ 2095, $\nu(\text{C}\equiv\text{CH})$ 3306 cm^{-1} . ^1H NMR (400 MHz, CDCl_3): $\delta = 7.31$ (d, $J = 3.8 \text{ Hz}$, 2H, Ar), 7.14 (d, $J = 3.8 \text{ Hz}$, 2H, Ar), 3.55 (s, 2H, $\text{C}\equiv\text{CH}$), 3.25–3.14 (m, 4H, $\text{CH}_3\text{C}_5\text{H}_{10}\text{CH}_2\text{CH}_2\text{CH}_2$), 1.93–1.85 (m, 4H, $\text{CH}_3\text{C}_5\text{H}_{10}\text{CH}_2\text{CH}_2\text{CH}_2$), 1.56–1.48 (m, 4H, $\text{CH}_3\text{C}_5\text{H}_{10}\text{CH}_2\text{CH}_2\text{CH}_2$), 1.37–1.27 (m, 20H, $\text{CH}_3\text{C}_5\text{H}_{10}\text{CH}_2\text{CH}_2\text{CH}_2$), 0.88 (t, $J = 6.6 \text{ Hz}$, 6H, $\text{CH}_3\text{C}_5\text{H}_{10}\text{CH}_2\text{CH}_2\text{CH}_2$) ppm. ^{13}C NMR (100 MHz, CDCl_3): $\delta = 194.99$, 187.31 (CO), 158.80, 156.44, 133.98, 131.33, 129.22, 129.09, 125.91 (Ar), 84.68, 75.69 ($\text{C}\equiv\text{C}$), 31.96, 31.65, 30.23, 29.54, 29.44, 29.37, 29.26, 22.80, 14.26 (C_9H_{19}) ppm. FAB-MS (m/z): 938 [$\text{M} + 1$] $^+$, 903 [$\text{M} - \text{Cl} + 1$] $^+$. Anal. Calc. For $\text{C}_{39}\text{H}_{44}\text{N}_2\text{ClO}_3\text{S}_4\text{Re}$: C, 49.90; H, 4.72; N, 2.98. Found: C, 49.88; H, 4.81; N, 3.05%.

L2-Re: Red solid (62%). **Spectral data:** IR (KBr): $\nu(\text{C}=\text{O})$ 1893br, 2015, $\nu(\text{C}\equiv\text{C})$ 2101, $\nu(\text{C}\equiv\text{CH})$ 3303 cm^{-1} . ^1H NMR (400 MHz, CDCl_3): $\delta = 7.23$ –7.19 (m, 6H, Ar), 7.11 (d, $J = 3.8 \text{ Hz}$, 2H, Ar), 3.47 (s, 2H, $\text{C}\equiv\text{CH}$), 3.30–3.16 (m, 4H, $\text{CH}_3\text{C}_5\text{H}_{10}\text{CH}_2\text{CH}_2\text{CH}_2$), 1.96–1.88 (m, 4H, $\text{CH}_3\text{C}_5\text{H}_{10}\text{CH}_2\text{CH}_2\text{CH}_2$), 1.57–1.51 (m, 4H, $\text{CH}_3\text{C}_5\text{H}_{10}\text{CH}_2\text{CH}_2\text{CH}_2$), 1.39–1.25 (m, 20H, $\text{CH}_3\text{C}_5\text{H}_{10}\text{CH}_2\text{CH}_2\text{CH}_2$), 0.87 (t, $J = 6.5 \text{ Hz}$, 6H, $\text{CH}_3\text{C}_5\text{H}_{10}\text{CH}_2\text{CH}_2\text{CH}_2$) ppm. ^{13}C NMR (100 MHz, CDCl_3): $\delta = 195.05$, 187.49 (CO), 158.47, 156.01, 140.21, 137.37, 134.24, 130.35, 129.56, 129.25, 125.22, 124.59, 122.41 (Ar), 83.34, 76.55 ($\text{C}\equiv\text{C}$), 32.01, 31.70, 30.23, 29.62, 29.49, 29.45, 29.31, 22.84, 14.27 (C_9H_{19}) ppm. FAB-MS (m/z): 1102 [$\text{M} + 1$] $^+$, 975 [$\text{M}-\text{Cl}+1$] $^+$. Anal. Calc. For

$C_{47}H_{48}N_2ClO_3S_6Re$: C, 51.18; H, 4.39; N, 2.54. Found: C, 51.30; H, 4.53; N, 2.79%.

2.3.2. Synthesis of platinum(II) metallopolyyne **P0-Re** to **P2-Re**

The polymers were prepared by the dehydrohalogenative polycondensation between *trans*-[Pt(PBu₃)₂Cl₂] [57] and each of **L0-Re** to **L2-Re**. A typical procedure was given for **P0-Re** starting from **L0-Re**.

Polymerization was carried out by mixing ligand **L0-Re** (40 mg, 0.05 mmol) and *trans*-[Pt(PBu₃)₂Cl₂] (35 mg, 0.05 mmol) in a 1:1 molar ratio in NEt₃/CH₂Cl₂ (20 mL, 1:2, v/v) and CuI (3 mg) was added to the mixture as a catalyst. After stirring at room temperature for 15 h under nitrogen, the solution mixture was evaporated to dryness. The residue was redissolved in a small volume of CH₂Cl₂, and filtered through a silica column using the same eluent to remove ionic impurities and catalyst residues. After removal of the solvent, the crude product was purified by precipitation from MeOH. Subsequent washing with *n*-hexane and drying *in vacuo* gave a red solid of **P0-Re** (50 mg, 93%).

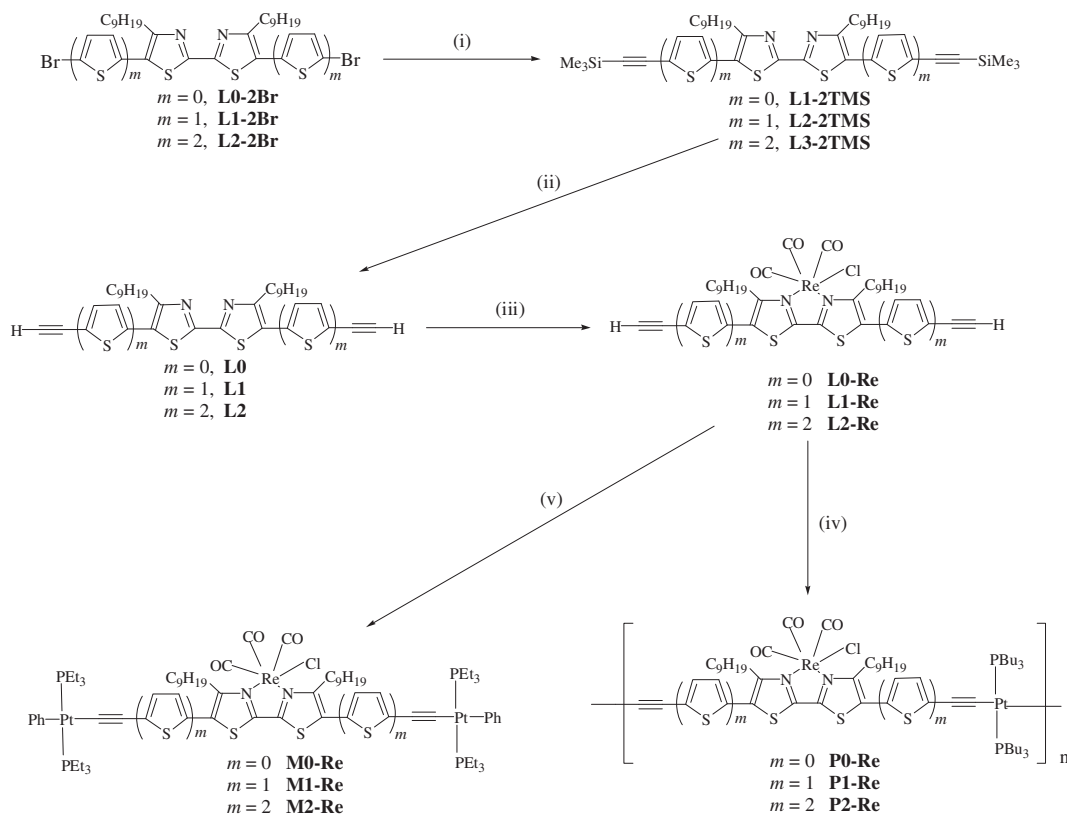
Spectral data: IR (KBr): $\nu(C=O)$ 1895, 1915, 2020, $\nu(C\equiv C)$ 2082 cm⁻¹. ¹H NMR (400 MHz, CDCl₃): δ = 3.07 (br, 4H, CH₃C₅H₁₀CH₂CH₂CH₂), 2.08 (br, 12H, PCH₂C₂H₄CH₃), 1.84 (br, 4H, CH₃C₅H₁₀CH₂CH₂CH₂), 1.56–1.47 (m, 28H, PCH₂C₂H₄CH₃ + CH₃C₅H₁₀CH₂CH₂CH₂), 1.27 (br, 20H, CH₃C₅H₁₀CH₂CH₂CH₂), 0.98–0.86 (m, 24H, PCH₂C₂H₄CH₃ + CH₃C₅H₁₀CH₂CH₂CH₂) ppm. ³¹P NMR (161 MHz, CDCl₃): δ = 4.27 (¹J_{P-Pt} = 2278 Hz) ppm. Anal. Calc. for (C₅₅H₉₂N₂ClO₃P₂S₂PtRe)_n: C, 48.14; H, 6.76; N, 2.04. Found: C, 48.32; H, 6.89; N, 2.12%. GPC (THF): M_w = 38490, M_n = 13170. PDI = 2.92.

P1-Re: Purple solid (93%). **Spectral data:** IR (KBr): $\nu(C=O)$ 1898, 1918, 2022, $\nu(C\equiv C)$ 2086 cm⁻¹. ¹H NMR (400 MHz, CDCl₃): δ = 7.05 (d, *J* = 3.8 Hz, 2H, Ar), 6.86 (br, 2H, Ar), 3.21–3.19 (m, 4H, CH₃C₅H₁₀CH₂CH₂CH₂), 2.13–2.11 (m, 12H, PCH₂C₂H₄CH₃), 1.89 (br, 4H, CH₃C₅H₁₀CH₂CH₂CH₂), 1.62–1.47 (m, 28H, PCH₂C₂H₄CH₃ + CH₃C₅H₁₀CH₂CH₂CH₂), 1.38–1.28 (m, 20H, CH₃C₅H₁₀CH₂CH₂CH₂), 0.97 (t, *J* = 7.2 Hz, 18H, PCH₂C₂H₄CH₃), 0.89 (t, *J* = 6.4 Hz, 6H, CH₃C₅H₁₀CH₂CH₂CH₂) ppm. ³¹P NMR (161 MHz, CDCl₃): δ = 3.70 (¹J_{P-Pt} = 2301 Hz) ppm. Anal. Calc. for (C₆₃H₉₆N₂ClO₃P₂S₄PtRe)_n: C, 49.25; H, 6.30; N, 1.82. Found: C, 49.40; H, 6.36; N, 2.02%. GPC (THF): M_w = 19810, M_n = 10760. PDI = 1.84.

P2-Re: Purple solid (86%). **Spectral data:** IR (KBr): $\nu(C=O)$ 1896, 1919, 2022, $\nu(C\equiv C)$ 2086 cm⁻¹. ¹H NMR (400 MHz, CDCl₃): δ = 7.16–7.11 (m, 4H, Ar), 7.05 (d, *J* = 3.6 Hz, 2H, Ar), 6.81 (br, 2H, Ar), 3.24–3.22 (m, 4H, CH₃C₅H₁₀CH₂CH₂CH₂), 2.14–2.11 (m, 12H, PCH₂C₂H₄CH₃), 1.92–1.90 (m, 4H, CH₃C₅H₁₀CH₂CH₂CH₂), 1.61–1.47 (m, 28H, PCH₂C₂H₄CH₃ + CH₃C₅H₁₀CH₂CH₂CH₂), 1.40–1.27 (m, 20H, CH₃C₅H₁₀CH₂CH₂CH₂), 0.97 (t, *J* = 7.2 Hz, 18H, PCH₂C₂H₄CH₃), 0.87 (t, *J* = 6.4 Hz, 6H, CH₃C₅H₁₀CH₂CH₂CH₂) ppm. ³¹P NMR (161 MHz, CDCl₃): δ = 3.61 (¹J_{P-Pt} = 2308 Hz) ppm. Anal. Calc. for (C₇₁H₁₀₀N₂ClO₃P₂S₆PtRe)_n: C, 50.14; H, 5.93; N, 1.65. Found: C, 50.32; H, 6.12; N, 1.86%. GPC (THF): M_w = 19900, M_n = 9220. PDI = 2.16.

2.3.3. Synthesis of platinum(II) model complexes **M0-Re** to **M2-Re**

All of them were synthesized following the dehydrohalogenative coupling between *trans*-[Pt(PEt₃)₂(Ph)Cl] [58] and the corresponding diterminal alkynes in a 2:1 ratio. A typical procedure was given for **M0-Re** starting from **L0-Re**.



Reagents and conditions: (i) trimethylsilylacetylene, Pd(OAc)₂, PPh₃, CuI; (ii) K₂CO₃, MeOH;

(iii) Re(CO)₅Cl, toluene, 60 °C; (iv) *trans*-[Pt(PBu₃)₂Cl₂], CuI, NEt₃; (v) *trans*-[Pt(PEt₃)₂(Ph)Cl], CuI, NEt₃

Scheme 1. Synthesis of rhenium(I)-bithiazole based diethynyl ligands **L0-Re** to **L2-Re** and their platinum(II) complexes **P0-Re** to **P2-Re** and **M0-Re** to **M2-Re**.

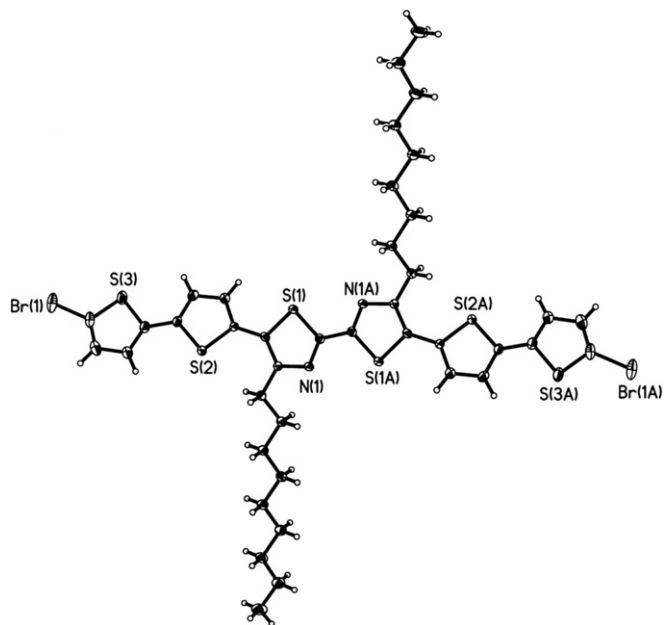


Fig. 2. X-ray crystal structure of **L2-2Br**, with thermal ellipsoids drawn at 25% probability levels. Labels on carbon atoms of the nonyl chains are omitted for clarity.

To a stirred mixture of ligand **L0-Re** (15 mg, 0.019 mmol) and 2 molar equivalents of *trans*-[Pt(PEt₃)₂(Ph)Cl] (21 mg, 0.038 mmol) in NEt₃ (15 mL) and CH₂Cl₂ (20 mL), CuI (3 mg) was added as a catalyst. The solution was stirred at room temperature for 15 h under nitrogen, after which all volatile components were removed under vacuum. The crude product was taken up in CH₂Cl₂ and purified on preparative silica TLC plates with a CH₂Cl₂/*n*-hexane mixture (3:1, v/v) as eluent. A red band consisting of **M0-Re** was obtained as a red solid (15 mg, 43%).

Spectral data: IR (KBr): $\nu(\text{C}=\text{O})$ 1894, 1913, 2019, $\nu(\text{C}\equiv\text{C})$ 2074 cm⁻¹. ¹H NMR (400 MHz, CDCl₃): δ = 7.32–7.24 (m, 4H, Ar), 7.01–6.98 (m, 4H, Ar), 6.85–6.81 (m, 2H, Ar), 3.07 (t, *J* = 8.2 Hz, 4H, CH₃C₅H₁₀CH₂CH₂CH₂), 1.86–1.68 (m, 28H, CH₃C₅H₁₀CH₂CH₂CH₂ + PCH₂CH₃), 1.53–1.46 (m, 4H, CH₃C₅H₁₀CH₂CH₂CH₂), 1.36–1.27 (m, 20H, CH₃C₅H₁₀CH₂CH₂CH₂), 1.14–1.06 (m, 36H, PCH₂CH₃), 0.88 (t, *J* = 6.6 Hz, 6H, CH₃C₅H₁₀CH₂CH₂CH₂) ppm. ¹³C NMR (100 MHz, CDCl₃): δ = 195.85, 188.49 (CO), 157.59, 154.47, 138.84, 136.73, 127.75, 123.15, 121.90 (Ar), 98.79 (C≡C), 32.02, 31.09, 30.41, 29.99, 29.84, 29.79, 29.50, 22.83, 15.24, 14.27, 8.13 (C₉H₁₉ + PEt₃) ppm. ³¹P NMR (161 MHz, CDCl₃): δ = 10.58 (¹*J*_{P-Pt} = 2613 Hz) ppm. FAB-MS (*m/z*): 1789 [M + 1]⁺. Anal. Calc. For C₆₇H₁₀₈N₂ClO₃P₄S₂Pt₂Re: C, 44.97; H, 6.08; N, 1.57. Found: C, 45.08; H, 6.15; N, 1.70%.

M1-Re: Purple solid (50%). **Spectral data:** IR (KBr): $\nu(\text{C}=\text{O})$ 1896, 1916, 2021, $\nu(\text{C}\equiv\text{C})$ 2080 cm⁻¹. ¹H NMR (400 MHz, CDCl₃): δ = 7.34–7.30 (m, 4H, Ar), 7.04 (d, *J* = 3.8 Hz, 2H, Ar), 7.00–6.97 (m, 4H, Ar), 6.85–6.81 (m, 4H, Ar), 3.25–3.18 (m, 4H, CH₃C₅H₁₀CH₂CH₂CH₂), 1.94–1.86 (m, 4H, CH₃C₅H₁₀CH₂CH₂ CH₂),

1.78–1.71 (m, 24H, PCH₂CH₃), 1.58–1.50 (m, 4H, CH₃C₅H₁₀CH₂CH₂CH₂), 1.39–1.26 (m, 20H, CH₃C₅H₁₀CH₂CH₂CH₂), 1.15–1.08 (m, 36H, PCH₂CH₃), 0.88 (t, *J* = 6.6 Hz, 6H, CH₃C₅H₁₀CH₂CH₂CH₂) ppm. ¹³C NMR (100 MHz, CDCl₃): δ = 195.32, 187.80 (CO), 157.30, 154.52, 139.00, 134.44, 130.73, 129.09, 127.83, 127.62, 125.94, 121.71 (Ar), 101.87 (C≡C), 32.03, 31.81, 30.24, 29.74, 29.63, 29.49, 29.43, 22.81, 15.24, 14.27, 8.18 (C₉H₁₉ + PEt₃) ppm. ³¹P NMR (161 MHz, CDCl₃): δ = 10.07 (¹*J*_{P-Pt} = 2619 Hz) ppm. FAB-MS (*m/z*): 1953 [M + 1]⁺. Anal. Calc. For C₇₅H₁₁₂N₂ClO₃P₄S₄Pt₂Re: C, 46.11; H, 5.78; N, 1.43. Found: C, 46.34; H, 5.89; N, 1.64%.

M2-Re: Purple solid (69%). **Spectral data:** IR (KBr): $\nu(\text{C}=\text{O})$ 1889, 1925, 2024, $\nu(\text{C}\equiv\text{C})$ 2080 cm⁻¹. ¹H NMR (400 MHz, CDCl₃): δ = 7.36–7.30 (m, 4H, Ar), 7.14 (d, *J* = 3.8 Hz, 2H, Ar), 7.10 (d, *J* = 3.8 Hz, 2H, Ar), 7.04 (d, *J* = 3.8 Hz, 2H, Ar), 7.00–6.96 (m, 4H, Ar), 6.84–6.78 (m, 4H, Ar), 3.28–3.19 (m, 4H, CH₃C₅H₁₀CH₂CH₂CH₂), 1.95–1.88 (m, 4H, CH₃C₅H₁₀CH₂CH₂CH₂), 1.78–1.71 (m, 24H, PCH₂CH₃), 1.58–1.53 (m, 4H, CH₃C₅H₁₀CH₂CH₂CH₂), 1.40–1.25 (m, 20H, CH₃C₅H₁₀CH₂CH₂CH₂), 1.15–1.07 (m, 36H, PCH₂CH₃), 0.88 (t, *J* = 7.0 Hz, 6H, CH₃C₅H₁₀CH₂CH₂CH₂) ppm. ¹³C NMR (100 MHz, CDCl₃): δ = 195.21, 187.64 (CO), 157.30, 155.32, 142.09, 139.09, 131.61, 131.42, 130.18, 130.12, 128.06, 127.56, 127.39, 124.90, 123.42, 121.61 (Ar), 102.30 (C≡C), 32.06, 31.70, 30.17, 29.62, 29.49, 29.43, 29.32, 22.82, 15.24, 14.27, 8.17 (C₉H₁₉ + PEt₃) ppm. ³¹P NMR (161 MHz, CDCl₃): δ = 10.04 (¹*J*_{P-Pt} = 2623 Hz) ppm. FAB-MS (*m/z*): 2117 [M + 1]⁺. Anal. Calc. For C₈₃H₁₁₆N₂ClO₃P₄S₆Pt₂Re: C, 47.07; H, 5.52; N, 1.32. Found: C, 47.22; H, 5.43; N, 1.44%.

2.3.4. X-ray crystallography

X-Ray diffraction data for **L2-2Br** were collected at 293 K using graphite-monochromated Mo-K α radiation (λ = 0.71073 Å) on a Bruker Axs SMART 1000 CCD diffractometer. The collected frames were processed with the software SAINT+ [59] and an absorption correction (SADABS) [60] was applied to the collected reflections. The structure was solved by the Direct or Patterson methods (SHELXTL) [61] in conjunction with standard difference Fourier techniques and subsequently refined by full-matrix least-squares analyses on *F*². Hydrogen atoms were generated in their idealized positions and all non-hydrogen atoms were refined anisotropically. Crystal data for **L2-2Br**·MeOH: C₄₁H₅₀N₂Br₂OS₆, *M_w* = 939.01, monoclinic, space group *P2/c*, *a* = 14.653(1), *b* = 4.1102(4), *c* = 37.163(4) Å, β = 92.642(2)°, *V* = 2235.8(4) Å³, *Z* = 2, ρ_{calcd} = 1.395 mg m⁻³, $\mu(\text{MoK}\alpha)$ = 2.126 mm⁻¹, *F*(000) = 968. 10008 reflections measured, of which 3843 were unique (*R*_{int} = 0.0348). Final *R*₁ = 0.0590 and *wR*₂ = 0.1428 for 2493 observed reflections with *I* > 2 σ (*I*).

3. Results and discussion

3.1. Synthetic methods and chemical characterization

The chemical structures of new platinum(II) polyyne polymers **P0-Re** to **P2-Re** and their well-defined model compounds **M0-Re** to **M2-Re** are shown in Scheme 1. Ligands **L0-Re** to **L2-Re** were prepared from **L0-L2** by reacting each of them with rhenium(I)

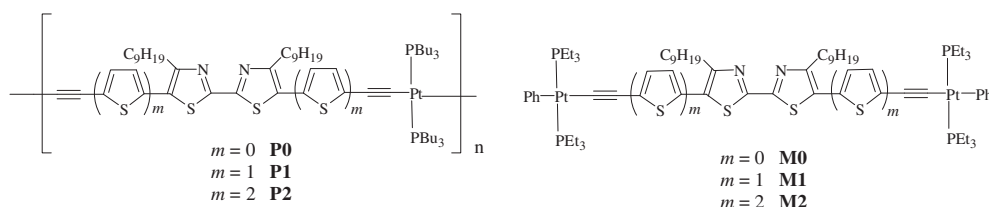


Fig. 3. Chemical structures of **P0-P2** and **M0-M2**.

Table 1
Electronic absorption and emission data of **L0-Re** to **L2-Re** and their corresponding metallated compounds.

	Absorption (293 K)		Emission (293 K)			
	λ_{abs} (nm)	CH_2Cl_2^a	Bandgap E_g [eV] ^b	λ_{em} (nm) CH_2Cl_2	Φ (%)	τ_p [ns]
L0-Re	229 (1.6), 257 (1.2)		2.59	467	c	c
	393 (2.0), 410 (2.1)			551		
L1-Re	230 (2.7), 275 (2.9)		2.27	498	c	c
	431 (3.7), 438 (3.7)			568		
L2-Re	230 (3.6), 350 (4.9)		2.08	611	c	c
	476 (4.5), 489 (4.4)					
M0-Re	231 (8.8), 304 (3.0)		2.23	565	0.05	1.18
	499 (6.0), 530 (6.8)					
M1-Re	231 (11.4), 349 (7.2)		1.95	652	0.19	0.60
	548 (6.0)					
M2-Re	230 (12.2), 388 (10.7)		1.87	712	0.14	0.55
	551 (6.5)					
P0-Re	230, 306, 539		2.18	582	0.05	0.22
P1-Re	229, 362, 548		1.95	659	0.09	0.44
P2-Re	229, 400, 552		1.85	729	0.10	0.34
L0	375 (2.47)		3.00	436	7.1	1.31
L1	296 (5.37), 413 (27.4)		2.55	493, 522	28.1	1.08
L2	337 (5.95), 440 (22.1)		2.38	539, 564*	22.8	1.28
M0	437 (5.1), 459* (4.6)		2.54	494, 517*	7.20	2.22
M1	332 (4.0), 463 (7.2)		2.29	560	9.40	1.70
M2	368 (7.3), 469 (12.8)		2.23	600	6.30	1.12
P0	452, 474		2.40	497	6.40	1.93
P1	346, 468		2.18	557	5.70	1.16
P2	378*, 476		2.10	592	5.10	1.34

Asterisk indicates a shoulder peak.

^a Molar extinction coefficients ($10^4 \text{ dm}^3 \text{ mol}^{-1} \text{ cm}^{-1}$) are shown in parentheses.

^b Optical bandgaps determined from the onset of absorption in solution phases.

^c Too weak to be determined accurately.

pentacarbonyl chloride using ethanol as the solvent at 60 °C. The Pt alkynyl compounds were prepared by the Sonogashira-type dehydrohalogenation between each of the diethynyl precursors (**L0-Re** to **L2-Re**) and suitable Pt chloride precursors [62–77]. The feed mole ratios of the platinum precursors and the diethynyl ligands were 1:1 and 2:1 for the polymer and dimer syntheses, respectively, and each product was carefully purified over silica gel to remove ionic impurities and catalyst residues. All of the Pt compounds are thermally- and air-stable solids and they are soluble in common chlorinated hydrocarbons and toluene. Gel-permeation chromatography (GPC) studies on **P0-Re** to **P2-Re** suggest their oligomeric/polymeric nature. The number-average molecular weights (M_n) of **P0-Re** to **P2-Re** calibrated against polystyrene standards range from 9220 to 13170 and **P0-Re** can

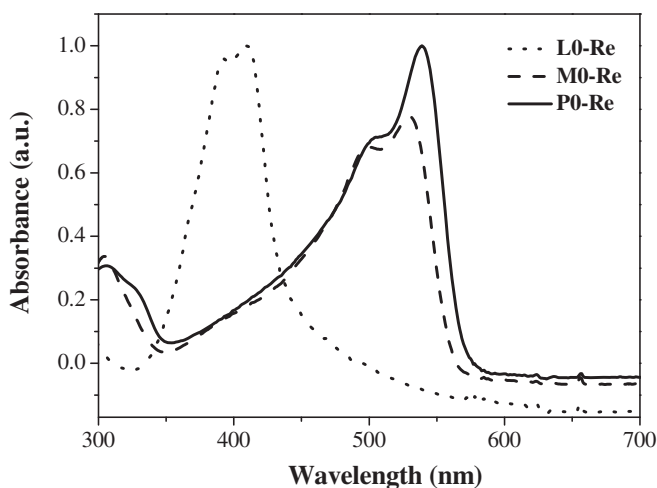


Fig. 4. Normalized absorption spectra of **L0-Re**, **M0-Re** and **P0-Re** at 293 K.

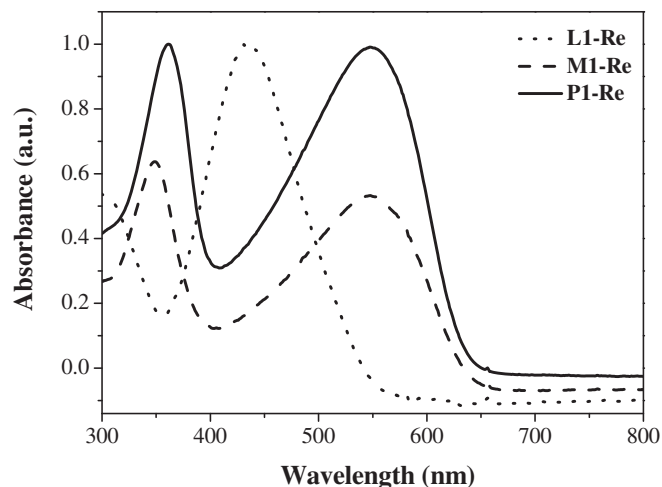


Fig. 5. Normalized absorption spectra of **L1-Re**, **M1-Re** and **P1-Re** at 293 K.

possess up to ~25 heterocyclic rings in total along the polymer chain based on M_n . The structures of these Pt compounds were unequivocally characterized using mass spectrometry, IR and NMR spectroscopies (see Experimental section). The NMR data are consistent with the proposed structures of the polymers and model compounds. The peaks arising from terminal $-\text{C}\equiv\text{CH}$ groups are absent in the NMR and IR spectra, confirming metal-alkynyl bond formation. From the crystal structure of **L2-2Br** shown in Fig. 2, it is clear that the molecule is essentially coplanar, consistent with a high degree of electronic π -conjugation.

The thermal properties of the polymers were also examined by thermal gravimetric analysis (TGA) under nitrogen. All of them exhibited good thermal stability with the decomposition onsets at around 303–329 °C, which are in general higher than those for *trans*- $[-\text{Pt}(\text{PBU}_3)_2\text{C}\equiv\text{CArC}\equiv\text{C}-]_n$ (Ar = C_6H_4 , 300 °C [78], anthrylene, 315 °C [79], oligothiophylene, 278–290 °C [64], etc.). Nevertheless, **P0-Re** to **P2-Re** tend to decompose more readily than the non-rhenium(I) congeners **P0–P2** (352–359 °C, Fig. 3). Decomposition onset was defined by a 5 wt.-% loss in each case.

3.2. Photophysical and electrochemical characterization

The photophysical data of all the compounds are summarized in Table 1. Figs. 4–6 show the absorption spectra of the metalloligands

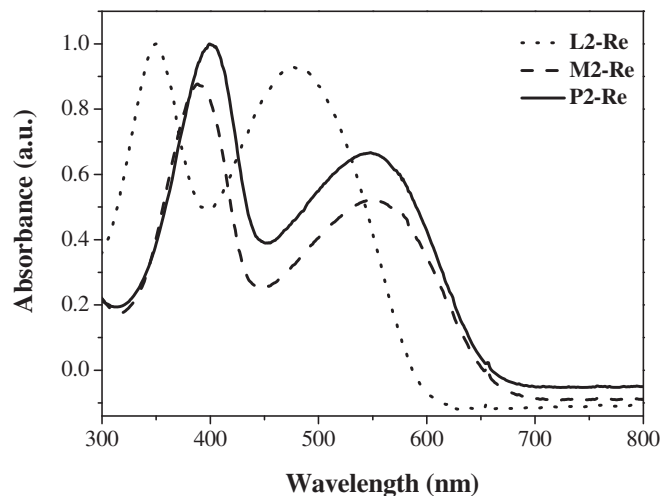


Fig. 6. Normalized absorption spectra of **L2-Re**, **M2-Re** and **P2-Re** at 293 K.

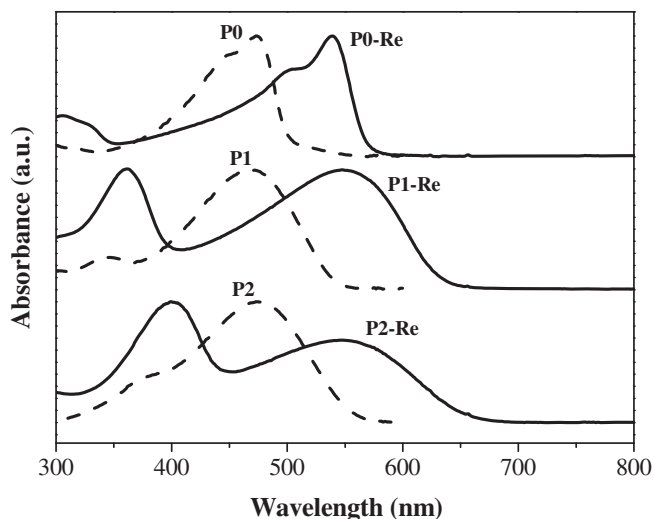


Fig. 7. Effect of coordination of the $\text{Re}(\text{CO})_3\text{Cl}$ group on the absorption profile.

L0-Re to **L2-Re** and their corresponding platinum(II) complexes. The absorption spectra of **P0-Re** exhibited an intense absorption band beyond 400 nm in the visible region, which is ascribed to the π - π^* transition of the conjugated spacer. Since there is no thienyl unit in **P0-Re** and **P0**, only one absorption band was observed. For **P1-Re** and **P2-Re**, two distinct chromophoric units were observed and their absorption spectra are dominated by two bands. The absorption peak at around 350–400 nm arises from the π - π^* transition of the oligothiophene segment whereas the broad strong absorption band in the visible region is ascribed to the intramolecular charge transfer (ICT) transition from the oligothiophene donor to the Re-bithazole acceptor. As the number of thienyl rings (m) increases from 1 to 2, the relative intensity of the first higher-energy band to the second lower-energy one also increases due to the increasing contribution of the thienyl absorption. Relative to the bithiazole based Pt polymers **P0–P2** without the $\text{Re}(\text{CO})_3\text{Cl}$ moiety, the absorption profiles of **P0-Re** to **P2-Re** experienced a clear red-shift in the spectral wavelengths [80,81] (Fig. 7). The absorption properties of **M0-Re**, **M1-Re** and **M2-Re** are very similar to those of **P0-Re**, **P1-Re** and **P2-Re**. There is hardly any further shift on going from the model compound to the polymer, indicating that the lowest singlet excited state is confined to a single repeat unit in the polymer chain [65]. Optical studies show that the pendant

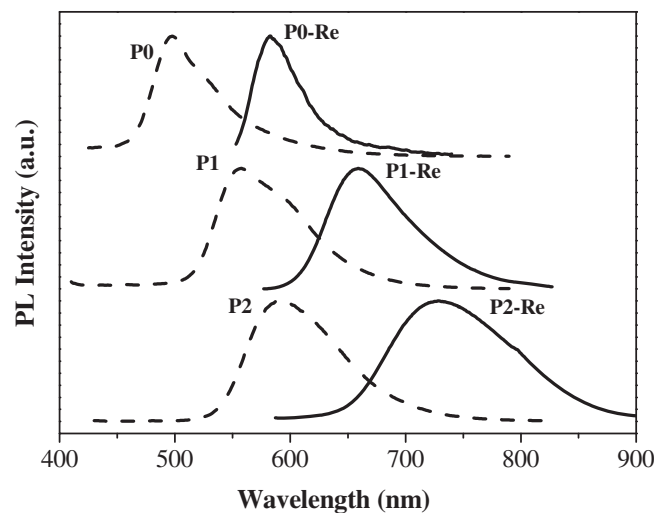


Fig. 9. Effect of coordination of the $\text{Re}(\text{CO})_3\text{Cl}$ group on the emission profile.

$\{\text{Re}(\text{CO})_3\text{Cl}\}$ fragment exerts an electron-withdrawing effect on the bithiazole core [80–82] such that the complexation of $\{\text{Re}(\text{CO})_3\text{Cl}\}$ with the bithiazole unit has greatly affected the electronic structure of the conjugated ligand as observed in the absorption spectra of **P0-Re** to **P2-Re**, relative to those of **P0** to **P2**.

Due to the presence of an extended π -electron delocalized system through the conjugated segment, the bandgaps for **P0–P2** range from 2.40 to 2.10 eV with increasing m value. By incorporating the electron-poor Re-bithiazole organic moiety into the electron-rich Pt metal center through the acetylenic groups, ICT can take place within the molecule from the metal group to the Re-bithiazole moiety. The bandgaps of **P0-Re** to **P2-Re** vary from 2.18 to 1.85 eV, where the absorption of **P2-Re** even tails off to 670 nm. In other words, we can easily manipulate the bandgaps of these bithiazole-linked polyplatinynes simply by coordination of the rhenium(I) unit to both nitrogen atoms.

Fig. 8 depicts the emission spectra of our Re-bithiazole based platinum(II) complexes and polymers. It was found that the emission intensity of **L0-Re** to **L2-Re** at 293 K is so weak that it is difficult to determine their lifetimes and quantum yields accurately. The Re-bithiazole based platinum complexes **M0-Re** to **M2-Re** (**P0-Re** to **P2-Re**) all emit strong featureless fluorescence from the singlet excited states at 565–712 nm (582–729 nm) with very short lifetimes (ca. 0.55–1.18 ns for model complexes and 0.22–0.44 ns for the polymers) under ambient conditions. We observed no phosphorescence emission from the triplet excited state over the measured spectral window for the polymers [65]. However, we cannot totally exclude the involvement of metal-to-ligand charge transfer excited state for the electronic transitions in **P0-Re** to **P2-Re**. Akin to the absorption data, there is a remarkable bathochromic shift in the emission profile of **P0-Re** to **P2-Re** after $\text{Re}(\text{CO})_3\text{Cl}$ group coordination (Fig. 9).

Besides, solvent effect on the spectral shift of the emission bands was studied for **P0-Re**, **P1-Re** and **P2-Re** (Table 2). From Figs. 10 and 11, the emission spectra of **P1-Re** and **P2-Re** exhibited

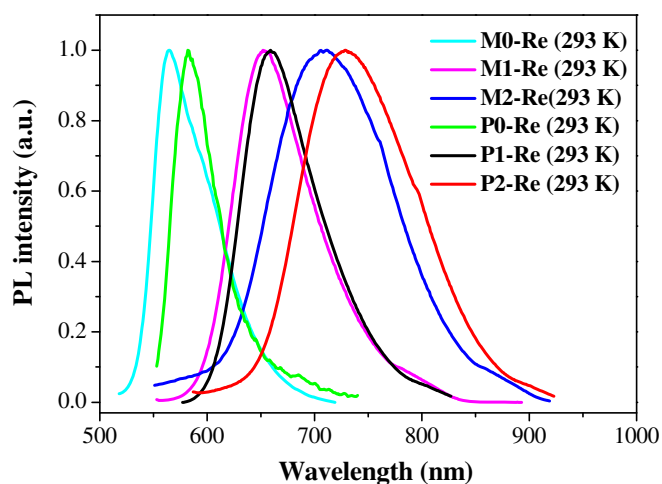


Fig. 8. Normalized emission spectra of **M0-Re** to **M2-Re** and **P0-Re** to **P2-Re**.

Table 2
Emission data [$\lambda_{\text{max,em}}$ (nm)] of **P0-Re**, **P1-Re** and **P2-Re** in different solvents at 293 K.

Solvent	Toluene	CHCl_3	THF	CH_2Cl_2
P0-Re	578	584	586	582
P1-Re	625	642	646	659
P2-Re	661	689	699	729

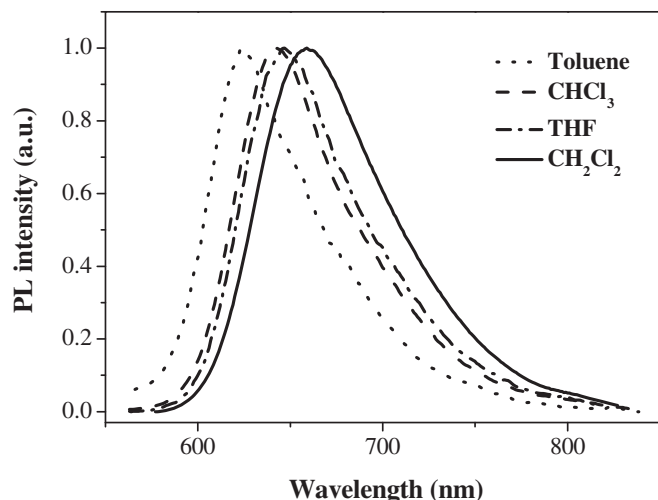


Fig. 10. Normalized emission spectra of **P1-Re** in different solvents at 293 K.

solvatochromic shifts in various solvents with different polarity, indicating their charge-transfer nature. The ICT emission peak of **P1-Re** spanned from 625 nm in toluene to 659 nm in CH_2Cl_2 . Likewise, the emission maxima of **P2-Re** were red-shifted from 661 nm in toluene to 729 nm in CH_2Cl_2 . This large red-shift ($\Delta\lambda = 34$ nm for **P1-Re** and 68 nm for **P2-Re**) shows that the difference of the dipole moment between the ground state and the excited state is significant. The bathochromic shift with increasing solvent polarity reveals that the ground state is less polar than the excited state (positive solvatochromism) [83,84]. Here, the shifts of the emission maximum with solvents are dramatic for **P1-Re** and **P2-Re** because the present system consists of alternating donor- π -acceptor structural units along the polymer chain and this agrees with our expectation for **P1-Re** and **P2-Re** exhibiting significant ICT interaction. Less apparent solvatochromism was observed in the fluorescence spectra of **P0-Re** (Table 2), because of the absence of the electron-donating thienyl rings to establish the donor-acceptor structure with the Re-bithiazole unit so that the ICT transition becomes less important in this case.

The highest occupied molecular orbital (HOMO) and the lowest unoccupied molecular orbital (LUMO) levels of our metallopolymer **P0-Re** to **P2-Re** were calculated using the redox

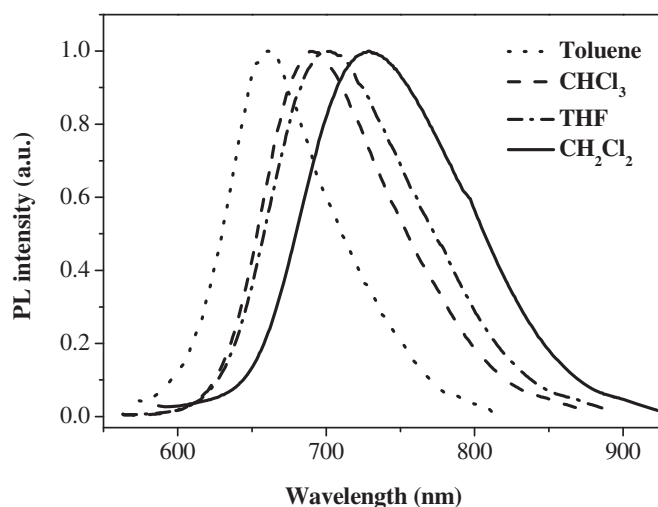


Fig. 11. Normalized emission spectra of **P2-Re** in different solvents at 293 K.

Table 3

Electrochemical data and frontier orbital energy levels for **P0-Re** to **P2-Re**.

Polymer	E_{ox} (V) ^a	E_{red} (V) ^a	E_{HOMO} (eV) ^b	E_{LUMO} (eV) ^b	E_{g}^{ec} (eV) ^c	$E_{\text{g}}^{\text{opt}}$ (eV) ^d
P0-Re	+1.35	-1.02	-6.07	-3.70	2.37	2.18
P1-Re	+1.27	-0.95	-5.99	-3.77	2.22	1.95
P2-Re	+1.14	-0.92	-5.86	-3.80	2.06	1.85

^a E_{ox} and E_{red} are the oxidation and reduction potentials, respectively.

^b $E_{\text{HOMO}} = -(E_{\text{ox}} + 4.72)$ eV and $E_{\text{LUMO}} = -(E_{\text{red}} + 4.72)$ eV.

^c E_{g}^{ec} = Electrochemical bandgap.

^d $E_{\text{g}}^{\text{opt}}$ = Optical bandgap.

potentials determined from electrochemical measurements using cyclic voltammetry. The experiments were performed by casting the polymer films on the glassy-carbon working electrode with a Ag/AgCl wire as the reference electrode, at a scan rate of 50 mV s^{-1} . The solvent in all measurements was deoxygenated MeCN, and the supporting electrolyte was 0.1 M $[\text{nBu}_4\text{N}]\text{BF}_4$. The relevant data are collected in Table 3. From the onset values of oxidation potential ($E_{\text{onset, ox}}$) and reduction potential ($E_{\text{onset, red}}$), the HOMO and LUMO levels of the polymers were calculated according to the following equations $E_{\text{HOMO}} = -(E_{\text{onset, ox}} + 4.72)$ eV and $E_{\text{LUMO}} = -(E_{\text{onset, red}} + 4.72)$ eV (where the unit of potential is V versus Ag/AgCl) [55,56]. It is evident that the presence of electron-donating thiophene on both sides of fluorene ring changes the electrical properties of the polymers. The cathodic wave is attributed to the reduction of bithiazole ring, which does not change much with the polymer structure. The thiophene ring mainly influences the oxidation potential of the polymer. The oxidation potential of **P0-Re** to **P2-Re** is reduced as a result of the thiophene ring extension, and each of them shows an irreversible thienyl oxidation at 1.35, 1.27 and 1.14 eV, respectively, which agrees with the phenomenon that formation of the heteroaromatic cation radicals is favored by increased conjugation length [85–91]. The electrooxidation of oligothiophenes is often irreversible because the electrogenerated cations readily undergo rapid coupling reactions leading to higher oligomers or polymers. The stability of these radical cations increases and the anodic wave becomes more reversible when m becomes longer [85–91]. Hence, the HOMO levels tend to be elevated with increasing m .

4. Conclusions

In summary, a new class of soluble, solution-processable heterobimetallic metallopolymer consisting of platinum(II) and rhenium(I) centers bridged by a bithiazole ring were prepared and characterized. Their small-molecular trinuclear model complexes were also studied for comparison. Optical spectroscopy and electrochemical data reveal narrow bandgap systems for **P0-Re** to **P2-Re** with the lowest gap value of 1.85 eV. Specially, a versatile approach has been developed toward controlling the bandgap and photophysical traits of polyplatinynes through chemical modification of the oligothiophene chain length as well as lateral complexation with a rhenium-tricarbonyl chloride pendant group. The photovoltaic effect of these low-bandgap polymers for the conversion of solar energy to electricity will form an interesting subject and such work will be carried out in the near future.

Acknowledgements

This work was supported by the Areas of Excellence Scheme, University Grants Committee of HKSAR, China (AoE/P-03/08), Hong Kong Research Grants Council (HKBU202607) and Hong Kong Baptist University (FRG2/09-10/091).

Appendix. Supplementary data

Supplementary data associated with this article can be found, in the online version, at doi:10.1016/j.jorganchem.2011.12.028.

References

- [1] J.J.M. Halls, C.A. Walsh, N.C. Greenham, E.A. Marseglia, R.H. Friend, S.C. Moratti, A.B. Holmes, *Nature (London)*, 376 (1995) 498–500.
- [2] F. Garnier, R. Haijalalou, A. Yassar, P. Srivastava, *Science* 265 (1994) 1684–1686.
- [3] J.R. Sheats, H. Antoniadis, M. Hueschen, W. Leonard, J. Miller, R. Moon, D. Roitman, A. Stocking, *Science* 273 (1996) 884–888.
- [4] N.J. Long, *Angew. Chem. Int. Ed. Engl.* 34 (1995) 21–38.
- [5] A.S. Abd-El-Aziz, E.K. Todd, *Coord. Chem. Rev.* 246 (2003) 3–52.
- [6] A.S. Abd-El-Aziz, C.E. Carraher, C.U. Pittman Jr., M. Zeldin Jr., *Macromolecules Containing Metal and Metal-Like Elements*, vol. 5, Wiley-Interscience, New Jersey, 2005.
- [7] W.-Y. Wong, *Dalton Trans.* (2007) 4495–4510.
- [8] W.-Y. Wong, X.-Z. Wang, Z. He, A.B. Djurišić, C.-T. Yip, K.-Y. Cheung, H. Wang, C.S.-K. Mak, W.-K. Chan, *Nat. Mater.* 6 (2007) 521–527.
- [9] W.-Y. Wong, *Macromol. Chem. Phys.* 209 (2008) 14–24.
- [10] I. Manners, *Synthetic Metal-Containing Polymers*, Wiley-VCH, Weinheim, 2004.
- [11] G.R. Whittell, M.D. Hager, U.S. Schubert, I. Manners, *Nat. Mater.* 10 (2011) 176–188.
- [12] K. Liu, C.-L. Ho, S. Aouba, Y.-Q. Zhao, Z.-H. Lu, S. Petrov, N. Coombs, P. Dube, H.E. Ruda, W.-Y. Wong, I. Manners, *Angew. Chem. Int. Ed.* 47 (2008) 1255–1259.
- [13] B.J. Holliday, T.M. Swager, *Chem. Commun.* 1 (2005) 23–36.
- [14] W.-Y. Wong, C.-L. Ho, *Acc. Chem. Res.* 43 (2010) 1246–1256.
- [15] C.-L. Ho, W.-Y. Wong, *Coord. Chem. Rev.* 255 (2011) 2469–2502.
- [16] G.-J. Zhou, W.-Y. Wong, *Chem. Soc. Rev.* 40 (2011) 2541–2566.
- [17] W.-Y. Wong, W.-K. Wong, P.R. Raithby, *J. Chem. Soc. Dalton Trans.* (1998) 2761–2766.
- [18] E.E. Havinga, W. Hoeve, H. Wynberg, *Synth. Met.* 55–57 (1993) 299–306.
- [19] J. Roncali, *Chem. Rev.* 97 (1997) 173–206.
- [20] C. Qin, Y. Fu, C.-H. Chui, C.-W. Kan, Z. Xie, L. Wang, W.-Y. Wong, *Macromol. Rapid Commun.* 32 (2011) 1472–1477.
- [21] X.-Z. Wang, Q. Wang, L. Yan, W.-Y. Wong, K.-Y. Cheung, A. Ng, A.B. Djurišić, W.-K. Chan, *Macromol. Rapid Commun.* 31 (2010) 861–867.
- [22] C.W. Tang, S.A. VanSlyke, *Appl. Phys. Lett.* 51 (1987) 913–915.
- [23] P.-T. Chou, Y. Chi, *Chem. Eur. J.* 13 (2007) 380–395.
- [24] W.-Y. Wong, C.-L. Ho, *Coord. Chem. Rev.* 253 (2009) 1709–1758.
- [25] G. Zhou, W.-Y. Wong, S. Suo, J. Photochem. Photobio. C: Photochem. Rev. 11 (2010) 133–156.
- [26] W.-Y. Wong, C.-L. Ho, *J. Mater. Chem.* 19 (2009) 4457–4482.
- [27] G. Zhou, W.-Y. Wong, X. Yang, *Chem. Asian J.* 6 (2011) 1706–1727.
- [28] R.C. Evans, P. Douglas, C. Winscom, *Coord. Chem. Rev.* 250 (2006) 2093–2126.
- [29] H. Wu, L. Ying, W. Yang, Y. Cao, *Chem. Soc. Rev.* 38 (2009) 3391–3400.
- [30] Y. Chi, *Chem. Soc. Rev.* 39 (2010) 638–655.
- [31] Y. You, S.Y. Park, *Dalton Trans.* (2009) 1267–1282.
- [32] Z.-J. Si, J. Li, B. Li, F.-F. Zhao, S.-Y. Liu, W.-L. Li, *Inorg. Chem.* 46 (2007) 6155–6163.
- [33] J.R. Shaw, R.H. Schmehl, *J. Am. Chem. Soc.* 113 (1991) 389–391.
- [34] S. Ranjan, S.-Y. Lin, K.-C. Hwang, Y. Chi, W.-L. Ching, C.-S. Liu, Y.-T. Tao, C.-H. Chien, S.-M. Peng, G.-H. Lee, *Inorg. Chem.* 42 (2003) 1248–1255.
- [35] M.A. Baldo, S. Lamansky, P.E. Burrows, M.E. Thompson, S.R. Forrest, *Appl. Phys. Lett.* 75 (1999) 4–6.
- [36] C. Adachi, M.A. Baldo, S.R. Forrest, M.E. Thompson, *Appl. Phys. Lett.* 77 (2000) 904–906.
- [37] J.C. Ostrowski, M.R. Robinson, A.J. Heeger, G.C. Bazan, *Chem. Commun.* (2002) 784–785.
- [38] Y. Ma, H. Zhang, J. Shen, C.-M. Che, *Synth. Met.* 94 (1998) 245–248.
- [39] S. Bernhard, X. Gao, *Adv. Mater.* 14 (2002) 433–436.
- [40] Y. Li, Y. Liu, J. Guo, F. Wu, W. Tian, B. Li, Y. Wang, *Synth. Met.* 118 (2001) 175–179.
- [41] A. Sarto Polo, M.K. Itokazu, N.Y.M. Iha, *Coord. Chem. Rev.* 248 (2004) 1343–1361.
- [42] S.-S. Sun, A.J. Lees, *J. Am. Chem. Soc.* 122 (2000) 8956–8967.
- [43] F.P.A. Johnson, M.W. George, F. Hartl, J. Turner, *Organometallics* 15 (1996) 3374–3387.
- [44] R. Alberto, R. Schibli, A. Egli, A.P. Schubiger, U. Abram, T.A. Kaden, *J. Am. Chem. Soc.* 120 (1998) 7987–7988.
- [45] W.-Y. Wong, S.-M. Chan, K.-H. Choi, K.-W. Cheah, W.-K. Chan, *Macromol. Rapid Commun.* 21 (2000) 453–457.
- [46] Q. Shi, H. Fan, Y. Liu, J. Chen, L. Ma, W. Hu, Z. Shuai, Y. Li, X. Zhan, *Macromolecules* 44 (2011) 4230–4240.
- [47] M. Zhang, H. Fan, X. Guo, Y. Yang, S. Wang, Z.-G. Zhang, J. Zhang, X. Zhan, Y. Li, *J. Polym. Sci. A: Polym. Chem.* 49 (2011) 2746–2754.
- [48] M. Zhang, H. Fan, X. Guo, Y. He, Z.-G. Zhang, J. Min, J. Zhang, G. Zhao, X. Zhan, Y. Li, *Macromolecules* 43 (2010) 8714–8717.
- [49] M. Zhang, H. Fan, X. Guo, Y. He, Z. Zhang, J. Min, J. Zhang, G. Zhao, X. Zhan, Y. Li, *Macromolecules* 43 (2010) 5706–5712.
- [50] T. Yamamoto, H. Suganuma, T. Maruyama, T. Inoue, Y. Muramatsu, M. Arai, D. Komarudin, N. Ooba, S. Tomaru, S. Sasaki, K. Kubota, *Chem. Mater.* 9 (1997) 1217–1225.
- [51] M. Karikomi, C. Kitamura, S. Tanaka, Y. Yamashita, *J. Am. Chem. Soc.* 117 (1995) 6791–6792.
- [52] W.-Y. Wong, K.-H. Choi, G.-L. Lu, Z. Lin, *Organometallics* 21 (2002) 4475–4481.
- [53] W.-Y. Wong, X.-Z. Wang, Z. He, K.-K. Chan, A.B. Djurišić, K.-Y. Cheung, C.-T. Yip, A.M.-C. Ng, Y.Y. Xi, C.S.-K. Mak, W.-K. Chan, *J. Am. Chem. Soc.* 129 (2007) 14372–14380.
- [54] C.-A. Fustin, P. Guillet, U.S. Schubert, J.-F. Gohy, *Adv. Mater.* 19 (2007) 1665–1673.
- [55] J. Hou, Z. Tan, Y. Yan, Y. He, C. Yang, Y. Li, *J. Am. Chem. Soc.* 128 (2006) 4911–4916.
- [56] C.G. Van de Walle, J. Neugebauer, *Nature (London)* 423 (2003) 626–628.
- [57] J. Chatt, R.G. Hayter, *J. Chem. Soc. Dalton Trans.* (1961) 896–904.
- [58] J. Chatt, B.L. Shaw, *J. Chem. Soc.* (1959) 4020–4033.
- [59] SAINT+, ver. 6.02a, Bruker, Analytical X-ray System, Inc, Madison, WI, 1998.
- [60] G.M. Sheldrick, SADABS, Empirical Absorption Correction Program, University of Göttingen, Germany, 1997.
- [61] G.M. Sheldrick, SHELXTL™, Reference Manual, ver. 5.1, Madison, WI, 1997.
- [62] A. Köhler, H.F. Wittmann, R.H. Friend, M.S. Khan, *J. Lewis, Synth. Met.* 77 (1996) 147–150.
- [63] A. Köhler, H.F. Wittmann, R.H. Friend, M.S. Khan, *J. Lewis, Synth. Met.* 67 (1994) 245–249.
- [64] N. Chawdhury, A. Köhler, R.H. Friend, W.-Y. Wong, J. Lewis, M. Younus, P.R. Raithby, T.C. Corcoran, M.R.A. Al-Mandhary, M.S.J. Khan, *J. Chem. Phys.* 110 (1999) 4963–4970.
- [65] M. Younus, A. Köhler, S. Cron, N. Chawdhury, M.R.A. Al-Mandhary, M.S. Khan, J. Lewis, N.J. Long, R.H. Friend, P.R. Raithby, *Angew. Chem. Int. Ed.* 37 (1998) 3036–3039.
- [66] A. Köhler, M. Younus, M.R.A. Al-Mandhary, P.R. Raithby, M.S. Khan, R.H. Friend, *Synth. Met.* 101 (1999) 246–247.
- [67] W.-Y. Wong, X.-Z. Wang, H.-L. Zhang, K.-Y. Cheung, M.-K. Fung, A.B. Djurišić, W.-K. Chan, *J. Organomet. Chem.* 693 (2008) 3603–3612.
- [68] L. Li, C.-L. Ho, W.-Y. Wong, K.-Y. Cheung, M.-K. Fung, W.-T. Lam, A.B. Djurišić, W.-K. Chan, *Adv. Funct. Mater.* 18 (2008) 2824–2833.
- [69] X.-Z. Wang, W.-Y. Wong, K.-Y. Cheung, M.-K. Fung, A.B. Djurišić, W.-K. Chan, *Dalton Trans.* (2008) 5484–5494.
- [70] N.J. Long, C.K. Williams, *Angew. Chem. Int. Ed.* 42 (2003) 2586–2617.
- [71] W.-Y. Wong, *J. Inorg. Organomet. Polym. Mater.* 15 (2005) 197–219.
- [72] S.J. Davies, B.F.G. Johnson, M.S. Khan, J.J. Lewis, *J. Chem. Soc. Chem. Commun.* (1991) 187–188.
- [73] J. Lewis, M.S. Khan, B.F.G. Johnson, T.B. Marder, H.B. Fyfe, F. Wittmann, R.H. Friend, *J. Organomet. Chem.* 425 (1992) 165–176.
- [74] Y. Fujikura, K. Sonogashira, N. Hagihara, *Chem. Lett.* (1975) 1067–1070.
- [75] K. Sonogashira, S. Takahashi, N. Hagihara, *Macromolecules* 10 (1977) 879–880.
- [76] K. Sonogashira, S. Kataoka, S. Takahashi, N.J. Hagihara, *J. Organomet. Chem.* 160 (1978) 319–327.
- [77] M.S. Khan, M.R.A. Al-Mandhary, M.K. Al-Suti, B. Ahrens, M.F. Mahon, L. Male, P.R. Raithby, C.E. Boothby, A. Köhler, *Dalton Trans.* (2003) 74–84.
- [78] W.-Y. Wong, C.-L. Ho, *Coord. Chem. Rev.* 250 (2006) 2627–2690.
- [79] M.S. Khan, M.R.A. Al-Mandhary, M.K. Al-Suti, F.R. Al-Battashi, S. Al-Saadi, B. Ahrens, J.K. Bjernemose, M.F. Mahon, P.R. Raithby, M. Younus, N. Chawdhury, A. Köhler, E.A. Marseglia, E. Tedesco, N. Feeder, S.J. Teat, *Dalton Trans.* (2004) 2377–2385.
- [80] C.S.K. Mak, W.K. Cheung, Q.Y. Leung, W.K. Chan, *Macromol. Rapid Commun.* 31 (2010) 875–882.
- [81] C.S.K. Mak, Q.Y. Leung, C.H. Li, W.K. Chan, *J. Polym. Sci. A: Polym. Chem.* 48 (2010) 2311–2319.
- [82] R.L. Cleary, K.L. Byrom, D.A. Bardwell, J.C. Jeffery, M.D. Ward, G. Calogero, N. Armaroli, L. Flamigni, F. Barigelletti, *Inorg. Chem.* 36 (1997) 2601–2609.
- [83] Z. Yuan, C.D. Entwistle, J.C. Collings, D. Albesa-Jove, A.S. Batsanov, J.A.K. Howard, N.J. Taylor, H.M. Kaiser, D.E. Kaufmann, S.-Y. Poon, W.-Y. Wong, C. Jardin, S. Fathallah, A. Boucekkinne, J.-F. Halet, T.B. Marder, *Chem. Eur. J.* 12 (2006) 2758–2771.
- [84] W.-Y. Wong, S.-Y. Poon, M.-F. Lin, W.-K. Wong, *Aust. J. Chem.* 60 (2007) 915–922.
- [85] P. Garcia, J.M. Pernaut, P. Hapiot, V. Wintgens, P. Valat, F. Garnier, D. Delabouglise, *J. Phys. Chem.* 97 (1993) 513–516.
- [86] I. Jestin, P. Frère, N. Mercier, E. Levillain, D. Stievenard, J. Roncali, *J. Am. Chem. Soc.* 120 (1998) 8150–8158.
- [87] A.F. Diaz, J. Crowley, J. Bargon, G.P. Gardini, J.B. Torrance, *J. Electroanal. Chem.* 121 (1981) 355–361.
- [88] Y. Harima, D.-H. Kim, Y. Tsutitori, X. Jiang, R. Patil, Y. Ooyama, J. Ohshita, A. Kunai, *Chem. Phys. Lett.* 420 (2006) 387–390.
- [89] I.F. Perepichka, D.F. Perepichka, H. Meng, F. Wudl, *Adv. Mater.* 17 (2005) 2281–2305.
- [90] R.D. McCullough, *Adv. Mater.* 10 (1998) 93–116.
- [91] T.-L. Stott, M.O. Wolf, *Coord. Chem. Rev.* 246 (2003) 89–101.